A major purpose of the Technical Information Center is to provide the broadest dissemination possible of information contained in DOE's Research and Development Reports to business, industry, the academic community, and federal, state and local governments.

Although a small portion of this report is not reproducible, it is being made available to expedite the availability of information on the research discussed herein.

1

LA-UR -84-1673

Los Alamos National Laboratory is operated by the University of California for the United States Department of Energy under contract W-7405-ENG-36

CONF-840804--17

TITLE: HEAT PIPE TECHNOLOGY DEVELOPMENT FOR HIGH TEMPERATURE SPACE RADIATOR APPLICATIONS

LA-UR--84-1673

DE84 012444

AUTHOR(S): M. A. Merrigan
E. S. Keddy
J. T. Sena
M. G. Elder

SUBMITTED TO: 19th Intersociety Energy Conversion Engineering Conference
San Francisco, California
August 19-24, 1984

Los Alamos National Laboratory
Los Alamos, New Mexico 87545

FORM NO 836 R4
ST NO 2629 5/81

HEAT PIPE TECHNOLOGY DEVELOPMENT FOR HIGH TEMPERATURE SPACE RADIATOR APPLICATIONS

M. A. Merrigan, E. S. Keddy, J. T. Sena, and M. G. Elder

Los Alamos National Laboratory, Los Alamos, New Mexico 87545

ABSTRACT

Technology requirements for heat pipe radiators, potentially among the lightest weight systems for space power applications, include flexible elements, and improved specific radiator performance(kg/kW). For these applications a flexible heat pipe capable of continuous operation through an angle of 180° has been demonstrated. The effect of bend angle on the heat pipe temperature distribution is reviewed. An analysis of light weight membrane heat pipe radiators that use surface tension forces for fluid containment has been conducted. The design analysis of these lightweight heat pipes is described and a potential application in heat rejection systems for space nuclear power plants outlined.

INTRODUCTION

Current developmental programs for space nuclear power systems have generated renewed interest in technology development for light weight, large area, heat rejection radiators with operating temperatures of greater than 600 K. Prime power systems now under study will require thermal rejection systems in the 2 to 100 megawatt range. Heat pipe radiators are potentially the lightest weight closed loop systems available in this power and temperature range and as such are baseline for most current studies. Technology requirements for the application of heat pipe radiators in these systems include the development of deployable structures in order to accommodate larger heat rejection areas than can be transported in deployed configuration. In addition, a need exists for improvement in specific radiator performance (kg/kW) through reduction in the weight of the structure.

In radiator design for space application a primary concern is the provision for end-of-life radiating area in the face of micrometeoroid damage threats. The conventional approach to ensuring sufficient heat transfer surface area at end-of-life is to armor the exposed surface of the radiator in order to ensure a reasonable probability that there will be no penetration of the surface by the micrometeroids over the life of the system. Optimization studies have shown that lighter weight, higher performance radiator designs are possible if the radiating surface is subdivided into independent segments before the required armor thickness is established. Improvements in performance by factors of two or more are possible by segmentation at realistic levels. This improvement in radiator performance by segmentation is seen both in tube and fin radiators where only the tube surface is armored, and in all-prime surface radiators where the entire surface must be protected. In either case, the underlying assumptions in conventional radiator design are that once a segment is penetrated by a micrometeroid, however small, it ceases to function and is lost to the system as far as heat rejection area is concerned. A primary advantage of heat pipe radiators in conventional designs of this type is that they lend themselves to the use of a high degree of segmentation with little weight penalty. Pumped liquid loop and gas loop radiators require additional complexity in order to achieve the same degree of segmentation.

Without segmentation the weight of armor required to ensure a 0.99 probability of survival in near earth orbit for a period of 10 years may be as much as 100 kg/m^2 for a radiator having an exposed area of 100 m^2 and using stainless steel as the material of construction (1) Subdividing the same 100 m^2 into 100 individual 1.0 m segments will reduce the armor requirement by about an order of magnitude. This represents about the limit for conventional radiator technology, with a specific weight of 6.0 to 10.0 kg/m^2 possible depending on the operating temperature and the resulting material requirements. Improvements in performance of conventional radiators are forseen in the development of lighter materials for use at higher temperatures and in the development of flexible heat transfer elements to permit folding of large surfaces for transport to their final operational orbit. Potentially higher gains in performance are possible through the development of advanced radiator concepts in which the heat transfer medium is, at least partially, exposed to space. In these concepts the penetration of the radiator area by a micrometeoroid is not assumed to result in automatic loss of the affected segment. Instead the effect of the penetration on the system is considered in terms of the size of the penetration and the resultant loss of heat transport medium. Loss of material to space is dependent on the surface area of fluid exposed, the vapor pressure and temperature of the working fluid, and on the action of other forces, such as surface tension, in controlling the movement of the material. Examples of advanced radiator concepts that are based on these concepts are the droplet and wetted belt radiators,(2) in both of which the entire quantity of heat transport fluid is exposed to space, and the rotating film and membrane heat pipe concepts, wherein the heat transport medium is exposed to space only at the micrometeoroid penetrations. The rotating film radiator concept, first discussed in Ref. (3), is the subject of another paper in this proceedings.(4) The membrane heat pipe is the subject of the present discussion.

Flexible Radiator Elements

The use of hard surfaced radiators for systems with reject heat loads in the megawatt range will require folding of the radiator surface for transport or assembly of the radiator structure in space. For unattended systems or those requiring assembly in higher orbits than are accessible to manned transportation systems, a remote deployment mechanism will be required. These deployment mechanisms will in general require the use of flexible elements in the heat transport path, functioning at power densitities in the range of kilowatts per centimeter squared. Flexible heat pipes, used for more than 15 years in lower temperature applications, are logical choices for this function. The technology requirements for fabrication of high power, flexible heat pipes capable of deployment through angles of up to 180 degrees, both cold and at temperature, exist. As a demonstration of this fact a flexible heat pipe employing sodium as a working fluid and using stainless steel wick and shell material has been assembled and tested. This device has been flexed repeatedly through angles of 180 degrees, both at room temperature with the sodium working fluid frozen and at temperatures to 1000 K while radiating heat to a room temperature environment. A cross section of the test heat pipe is shown in Fig. 1. The wick structure is composed of three layers of 100 mesh stainless steel screen wrapped on a bias in alternating directions. The corrugated portion of the heat pipe is fabricated from a standard high vacuum flexible line section. The heated (evaporator) length is 15 cm, flexible length 45 cm, and the remainder of the condenser region 20 cm.

Demonstration of Flexible Heat Pipe

Initial testing of the flexible heat pipe

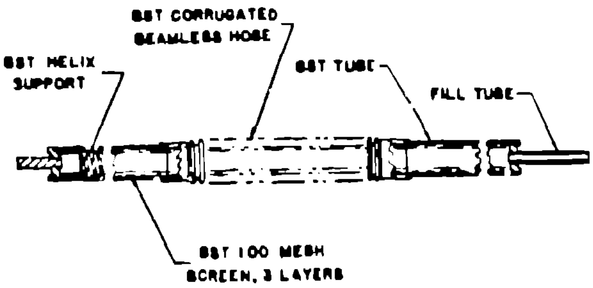

Fig. 1. Cross section of flexible heat pipe.

involved operation at a temperature of 1000 K in a horizontal position, then elevation of the condenser end of the heat pipe upward through an arc until a bend of 180 degrees in the vertical plane was achieved. Heat pipe operation through the bending operation and in the flexed position was verified by visual inspection. Following this operational demonstration, instrumentation was installed to determine the effective emissivity of the radiating surface and the total power throughput of the heat pipe. A single pass quartz calorimeter was placed around the heat pipe and type K thermocouples welded to the pipe surface at intervals to measure axial temperature variation. Initially the heat pipe was operated with the calorimeter evacuated. Heat throughput was determined from water flow and temperature change measurements. Surface emissivity of the heavily oxidized stainless steel heat pipe surface was determined to be 0.49 in these tests. Following this determination the heat pipe was removed from the calorimeter and testing continued in air. In these tests the heat losses from the evaporator section of the heat pipe were subtracted from the calculated power in order to arrive at power throughput. In tests to determine this effect of bend angle on the heat pipe performance the heat pipe was operated with the bend in the horizontal plane. Bend tests were conducted in three stages. The heat pipe was operated in a straight and level position and axial temperatures were recorded as a function of power. Next the heat pipe was operated with a 90° bend at a bend radius of 28 cm with temperatures recorded for the same power levels. Finally the heat pipe was bent through 180° with a bend radius of 14 cm and the process repeated. Figure 2 presents the results of these measurements as a plot of the axial delta T of the heat pipe from the evaporator exit to the end of the condenser as a function of the bend angle for power levels of 1550 and 2000 watts. While these data indicate a significant increase in axial temperature drop due to the bending no loss of heat pipe function was observed under test power throughput to 1950 W/cm^2. In addition the heat pipe was repeatedly started from below the freezing point of the sodium result in automatic loss of the affected segment. Instead the effect of the penetration on the system is considered in terms of the size of the penetration and the resultant loss of heat transport medium. Loss of material to space is dependent on the surface area of fluid exposed, the vapor pressure and temperature of the working fluid, and on the action of other forces, such as surface tension, in controlling the movement of the material. Examples of advanced radiator concepts that are based on these concepts are the droplet and wetted belt radiators,(2) in both of which the entire quantity of heat transport fluid is exposed to space, and the rotating film and membrane heat pipe concepts, wherein the heat transport medium is exposed to space only at the micrometeroid penetrations. The rotating film radiator concept, first discussed in Ref. (3), is the subject of another paper in this proceedings.(4) The membrane heat pipe is the subject of the present discussion.

Flexible Radiator Elements

The use of hard surfaced radiators for systems with reject heat loads in the megawatt range will require folding of the radiator surface for transport or assembly of the radiator structure in space. For unattended systems or those requiring assembly in higher orbits than are accessible to manned transportation systems, a remote deployment mechanism will be required. These deployment mechanisms will in general require the use of flexible elements in the heat transport path, functioning at power densitities in the range of kilowatts per centimeter squared. Flexible heat pipes, used for more than 15 years in lower temperature applications, are logical choices for this function. The technology requirements for fabrication of high power, flexible heat pipes capable of deployment through angles of up to 180 degrees, both cold and at temperature, exists. As a demonstration of this fact a flexible heat pipe employing sodium as a working fluid and using stainless steel wick and shell material has been assembled and tested. This device has been flexed repeatedly through angles of 180 degrees, both at room temperature with the sodium working fluid frozen and at temperatures to 1000 K while radiating heat to a room temperature environment. A cross section of the test heat pipe is shown in Fig. 1. The wick structure is composed of three layers of 100 mesh stainless steel screen wrapped on a bias in alternating directions. The corrugated portion of the heat pipe is fabricated from a standard high vacuum flexible line section. The heated (evaporator) length is 15 cm, flexible length 45 cm, and the remainder of the condenser region 20 cm.

Demonstration of Flexible Heat Pipe

Initial testing of the flexible heat pipe

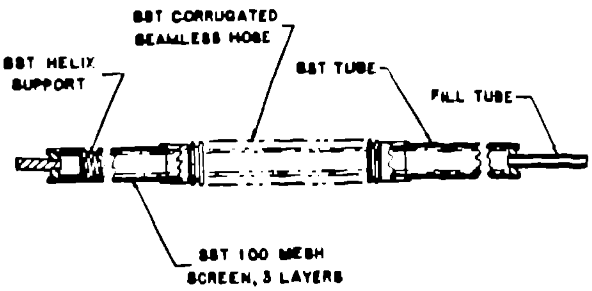

Fig. 1. Cross section of flexible heat pipe.

involved operation at a temperature of 1000 K in a horizontal position, then elevation of the condenser end of the heat pipe upward through an arc until a bend of 180 degrees in the vertical plane was achieved. Heat pipe operation through the bending operation and in the flexed position was verified by visual inspection. Following this operational demonstration, instrumentation was installed to determine the effective emissivity of the radiating surface and the total power throughput of the heat pipe. A single pass quartz calorimeter was placed around the heat pipe and type K thermocouples welded to the pipe surface at intervals to measure axial temperature variation. Initially the heat pipe was operated with the calorimeter evacuated. Heat throughput was determined from water flow and temperature change measurements. Surface emissivity of the heavily oxidized stainless steel heat pipe surface was determined to be 0.49 in these tests. Following this determination the heat pipe was removed from the calorimeter and testing continued in air. In these tests the heat losses from the evaporator section of the heat pipe were subtracted from the calculated power in order to arrive at power throughput. In tests to determine this effect of bend angle on the heat pipe performance the heat pipe was operated with the bend in the horizontal plane. Bend tests were conducted in three stages. The heat pipe was operated in a straight and level position and axial temperatures were recorded as a function of power. Next the heat pipe was operated with a 90° bend at a bend radius of 28 cm with temperatures recorded for the same power levels. Finally the heat pipe was bent through 180° with a bend radius of 14 cm and the process repeated. Figure 2 presents the results of these measurements as a plot of the axial delta T of the heat pipe from the evaporator exit to the end of the condenser as a function of the bend angle for power levels of 1550 and 2000 watts. While these data indicate a significant increase in axial temperature drop due to the bending no loss of heat pipe function was observed under test power throughput to 1950 W/cm^2. In addition the heat pipe was repeatedly started from below the freezing point of the sodium working fluid without any apparent adverse effects due to bend angle.

CONCEPT DESCRIPTION
MEMBRANE HEAT PIPE RADIATOR

An alternative to the combination of armor and segmentation used to ensure end-of-life heat transport capability in conventional heat pipe radiators is to abandon the use of armor entirely and let the material thicknesses used in the heat pipe assembly be determined by strength and fabrication considerations only. In this scheme preservation of end-of-life area requirements is accomplished through a high degree of segmentation with the segment area determined by the size of the largest micrometeoroid penetration expected over the life of the system. If this maximum hole size is such as to contain the working fluid at its operating conditions through the action of surface tension, then the loss of fluid from the system will be a result of evaporation from the area of the punctures only. Segments that suffer a penetration larger than this surface tension limit determined value will lose their working fluid by its being forced through the opening and into space under the influence of the internal pressure, corresponding to the equilibrium vapor pressure of the working fluid at the operating temperature of the radiator.

This concept has a number of benefits in addition to the basic concern for reduced weight per unit area. Loss of working fluid from the radiator assembly will be much lower than for those advanced radiator concepts in which the entire quantity of working fluid is exposed to space. This will reduce the weight of fluid that must be carried in the system for make-up but more importantly it will reduce the hazards of contamination of the remainder of the space craft by the escaping fluid. A second important consideration will be that the thin material sections required for containment of the working fluid in the unarmored configuration will lend themselves to the development of flexible structures, inherently capable of compact storage and deployment in space. In the limit one may consider structures that are passively deployed by the internal pressure developed as the working fluid is brought to the operating temperature and thus requiring no linkages, actuators, or special purpose elements for deployment. Such a concept is shown in Fig. 3, where a flat array of membrane heat pipes, joined to form a sheet structure, is rolled into a cylindrical configuration for transport aboard the launch vehicle and unrolled in space to form the radiator surface. The analysis that follows assumes that the radiator surface is exposed throughout the life of the system. However, for intermittently operated systems it would be possible to maintain the radiating surface in its stowed configuration when the system is not operating and greatly reduce the effects of the micrometeoroid environment.

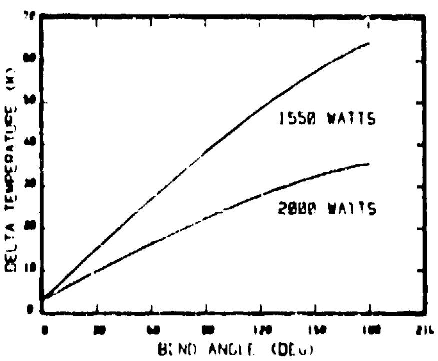

Fig. 2. ΔT between evaporator exit and end of condenser versus bend angle of heat pipe.

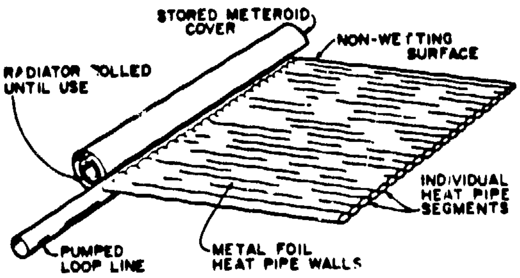

Fig. 3. Self deployed membrane heat pipe radiator concept.

MEMBRANE RADIATOR ANALYSIS

The National Aeronautics and Space Administration (NASA) Near Earth to Lunar Surface Meteoroid Environment Model(5) was chosen for use in this analysis. In this model the near-Earth average total meteoroid (average sporadic plus average stream) mass-flux is given by:

$$\log_{10} N_t = -14.37 - 1.213 \log_{10} m, \quad \text{for } 10^{-6} \le m \le 1. \qquad (1)$$

where: N_t = number of particles of mass m or greater per m^2-s and
m = particle mass (g).

The assumed average particle density and velocity for this model are 0.5 g/cm^3 and 20 km/s. Correction for the Earths gravitational effect is accomplished by multiplying N_t by a defocusing factor, G_e, which ranges from 1.0 at the Earth's surface to about 0.57 at infinity. The shielding effect of the earth is similarly accounted for by a shielding factor E, defined by $E = (1+\cos\theta)/2$, where 2θ = the angle subtended by the Earth as viewed from the spacecraft. For this analysis G_e is taken as 1.0 and E as 0.75, corresponding to the case of a 700 to 800 km orbit.

The probability of impact of the radiator by n particles of mass m or greater is determined from the Poisson distribution equation,

$$P_{(x \leq n)} = \sum_{r=v}^{r=n} \frac{e^{N_t A \tau} (N_t A \tau)^r}{r!} \quad , \qquad (2)$$

where

- $P_{(x \leq n)}$ = probability of impact by n meteoroids or less,
- n_t = particle flux (particles/m^2-s),
- A = exposed area (m^2), and
- τ = exposure time.

This expression may be used with the area of an individual radiator segment to determine the maximum hole size expected at some probability at end-of-life. For this analysis an 0.99 probability of no larger punctures in a 7-year period is assumed, resulting in the variation of maximum hole diameter with segment area given in Fig. 4. The two curves represent an upper limit based on a hemispherical cavity with radius equal to the semi-infinite penetration thickness of a particle and a lower limit at the diameter of the impacting particle. For very thin material sections the values will approach the lower curve.

In order to determine what hole diameter is tolerable for containment of the heat pipe working fluid by surface tension forces the internal pressure is set equal to the surface force developed at the hole,

$$P_v \leq \frac{4\sigma}{D} \qquad (3)$$

where,

- P_v = equilibrium vapor pressure of the working fluid (dyne/cm^2),
- σ = surface tension (dyne/cm), and
- D = maximum penetration diameter (cm),

with all properties evaluated at the radiator operating temperature. A plot of the resulting maximum allowable penetration diameter is given in Fig. 5. These data establish a practical upper operating temperature limit for the case considered at the point where the area of an individual segment becomes impractically small. The lower temperature limit for operation with a particular heat pipe working fluid will be established by the sonic limit criteria.(6) That is, the cross sectional area available for vapor flow in the heat pipe must be greater than that required to transport the design heat load at the sonic velocity limit in the vapor. The maximum axial flux density is shown in Fig. 6 for various liquid metal working fluids based on the sonic limit.

If cylindrical geometry is assumed the heat pipe proportions may be determined from an assumed surface emissivity, the operating temperature, and the allowable axial flux density. If we neglect the wick area the limiting heat flux into the radiating section of the heat pipe will be,

$$Q_{in} = (q_s)\, \pi\, D^2/4, \qquad (4)$$

and the radiated energy will be

$$Q_r = \sigma\, \varepsilon\, \pi\, D\, L\, T^4, \qquad (5)$$

where:
- q_s = sonic power limit (w/cm^2)
- D = heat pipe diameter (cm)
- L = heat pipe length (cm)

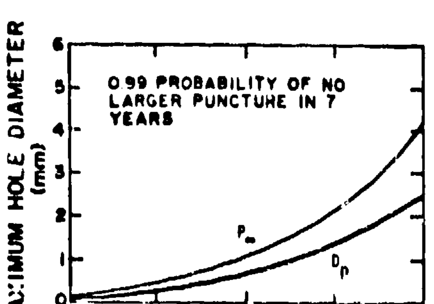

Fig. 4. Maximum micrometeoroid penetration diameter as a function of radiator segment area.

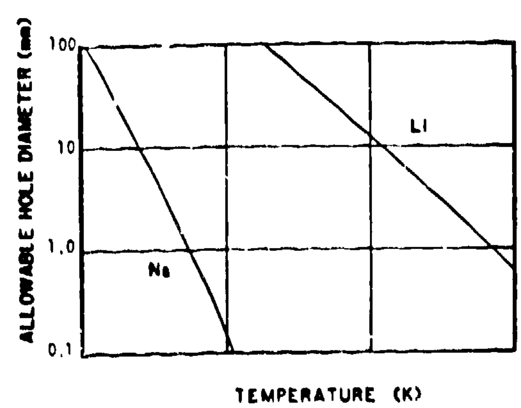

Fig. 5. Allowable penetration diameter for surface tension containment of heat pipe working fluid.

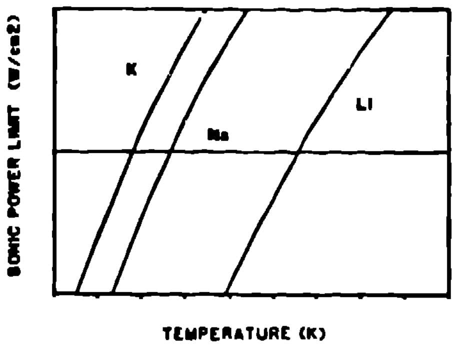

Fig. 6. Sonic power limit for alkali metal heat pipe fluids.

ε = surface emissivity
σ = Stefan-Boltzmann constant (5.6686×10^{-12} W/cm T^4).

Equating input and output,

$$\frac{D}{L} = \frac{4 \varepsilon \sigma T^4}{q_s} \quad . \tag{6}$$

determines the heat pipe proportions.

An additional concern in the design of heat pipe radiator elements for these applications will be the quantity of fluid lost from the heat pipes over the life of the system. This is determined by calculating the total area of the meteroid punctures per unit area of surface for those radiator elements whose maximum meteoroid hole is within the range where surface tension will contain the fluid. The range of hole sizes will vary from this upper value to a minimum established by the heat pipe containment thickness and type of material. The Charters and Summers (C-S)(7) equation is used to predict the minimum particle size for penetration.

$$P_\infty = \frac{81}{8\pi}\left(\frac{\rho_p}{\rho_t}\, m_p\, u_p^2\right)^{1/3} \frac{1}{S_t^{1/3}} \tag{7}$$

where P_∞ = penetration in a semi-infinite solid (mm)
m_p = meteoroid mass (kg)
U_p = meteoroid velocity (20 km/s)
ρ_p = meteoroid density (0.5 g/cm^3)
ρ_t = target material density (g/cm^3)
$S_t^{1/3}$ = target material factor (J/mm^3)$^{1/3}$

The material property factor in the C-S equation, $S_t^{1/3}$ is determined experimentally, with values in the range of 3 to 4 for beryllium, titanium, and stainless steels at temperatures to 775 K.(8-9) The total penetration thickness (TPT) defined as that thickness of material that will just prevent penetration of a given size of particle, is taken as 1.5 p_∞ based on the previously cited hypervelocity impact studies. When the range of penetrating meteoroid masses has been determined the total area of the resulting holes may be determined from the assumed particle density and the meteoroid mass flux model.

Figure 7 presents the total meteoroid hole area as a function of surface sheet thickness for a 316 stainless steel radiator surface at end-of-life for a 7-year exposure in a 700 to 800 km orbit.

The fluid loss from a heat pipe is given by

$$G = 5.833 \times 10^{-2}\ P_v \left(\frac{M}{T}\right)^{1/2} \tag{8}$$

where

G = mass loss rate (g/cm^{2}s)
P_v = vapor pressure of the working fluid (mm Hg)
m = molecular mass of the working fluid (g)
T = temperature (K)

The amount of working fluid lost from a heat pipe over the life of the system will be

$$M = G\,A\,t$$

where A = heat pipe surface area (cm^2)
t = exposure time (s)

The heat pipe must be designed to function with this quantity of surplus fluid at beginning-of-life.

Design Example

A 100 MW$_t$ radiator operating at 1000 K is considered. The heat pipe structures are assumed to be formed of 0.1 mm, 316 stainless steel foil with wicking provided by surface texturing and lithium used as a working fluid. The radiator is assumed to be segmented to a level of 0.5 m^2/heat pipe. The 0.99 probability maximum penetration diameter at end-of-life, assuming a 7 year exposure, is ~ 0.5 mm from Fig. 4. The maximum allowable hole size for surface tension containment is 10 mm from Fig. 5. The resulting diameter to length ratio, from Eq. (6), will be 0.19. For the assumed segment area this will correspond to a heat pipe 0.17 m in diameter and 0.92 m in length.

Total area of meteoroid penetrations after 7 years exposure will be approximately 15 mm^2 from Fig. 7 and the fluid mass loss rate from the heat pipe will be

$$G_t = 4.67 \times 10^{-3}\ \text{gm/cm}^2\ \text{s}$$

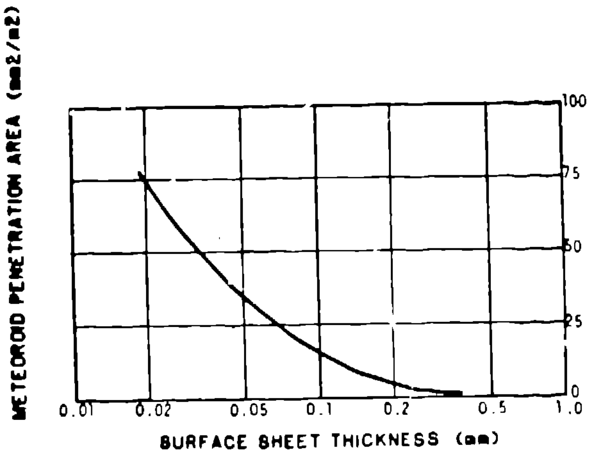

Fig. 7. Total meteoroid penetration area after a 7-yr exposure as a function of surface sheet thickness of 316 SS.

at 1000 K. The normal lithiu fill quantity for this size of heat pipe would be about 50 gm. It if is assumed that the heat pipe can be operated initially with a 100% overfill, then the working fluid reserve for evaporation losses will be about 50 gm and tne corresponding period of operation at 1000 K will be 8.9 x 10^4 s or about 24 hours. The heat pipes could be operated for longer periods at lower temperatures, however the sonic power limit would impose a severe restriction. The more promising approach to longer term operation would be to shield the radiator surface in its transport configuration and deploy only during periods of system operation.

Estimated weight for this design example will be

Containment	388 gm
Wicking (arteries)	20 gm
Lithium working charge	50 gm
Lithium evaporation loss	50 gm
Distribution line/heat pipe	300 gm
	806 gm

Allowing a 20% design margin for array losses by penetrations larger than the surface tension limit, the radiation specific weight will be 1.8 kg/m^2 or about 0.04 kg/kW at 1000 K. This compares favorably with other advanced radiator concepts.

CONCLUSIONS

It has been demonstrated that flexible sodium/stainless steel heat pipes can be fabricated and operated at temperatures to 1100 K with axial throughputs of 1950 W/cm^2. It has also been demonstrated that this type of heat pipe can be flexed up to 180 degrees while at temperature and under load. Start up of these heat pipes from below the freezing temperature of sodium has been demonstrated for bend positions up to 180° in a nongravity assisted mode of operation.

The membrane heat approach to space power system radiator design has been examined and found to be of potential value in systems designed for intermittent operation. Radiator performance levels of 0.04 kg/kW appear possible for integrated operating times of 24 hours at 1000 K after 7-years exposure to near Earth meteoroid flux levels. Perhaps the most attractive characteristic of the membrane heat pipe radiator concept would be its capability for use in flexible arrays that may be compactly stowed for transport by rolling or folding.

REFERENCES

1. D. G. Elliott, "External Flow Radiators for Reduced Space Powerplant Temperatures," 1st Symposium on Space Nuclear Power Systems," January 1984.

2. K. K. Knapp, "Lightweight Moving Radiators for Heat Rejection in Space," AIAA 16th Thermophysics Conference, June 1981.

3. F. C. Prenger and J. A. Sullivan, "Conceptual Designs for 100 MW Space Radiators," National Academy of Sciences Symposium on Advanced Compact Reactors, November 1982.

4. D. R. Koenig, "Light-Weight Rotating Film Radiators," Proceedings IECEC 84.

5. B. G. Cour-Palais, "Meteoroid Environment Model - 1969," NASA report NASA-SP-8013, March 1969.

6. P. D. Dunn and D. A. Reay, "Heat Pipes," Pergamon Press, Oxford, 1978.

7. E. Schneider, "Velocity Dependence of Some Impact Phenomena," ESA Halley Comet Micrometeoroid Hazard Workshop, Nordwijk, April 1979.

8. N. Clough, S. Lieblein, and A. McMillan, "Crater Characteristics of 11 Metal Alloys Under Hyper-Velocity Impact," NASA TN-D-5135, April 1969.

9. L. Lundberg, S. Bless, S. Girrens, J. Green, "Hypervelocity Impact Studies on Titanium, Titanium Alloys, and Beryllium," Los Alamos National Laboratory LA-9417-MS, August 1982.